RNA (1996), 2:937–955. Cambridge University Press. Printed in the USA.

Secondary and tertiary structure in the central domain of adenovirus type 2 VA RNA_I

YULIANG MA[1,2,3] and MICHAEL B. MATHEWS[1]

[1] Cold Spring Harbor Laboratory, Cold Spring Harbor, New York 11724, USA
[2] Molecular Microbiology Program, State University of New York, Stony Brook, New York 11790, USA

ABSTRACT

The small (160 nt) adenovirus RNA, VA RNA_I, antagonizes the activation of the cellular protein kinase PKR (also known as DAI), a key regulator of gene expression. VA RNA consists of two stems separated by a complex region, the central domain, that is essential for its function. A notable feature of the central domain is a pair of tetranucleotides, GGGU and ACCC, which are mutually complementary and phylogenetically conserved. To investigate their role in the structure and function of VA RNA, we generated three sets of mutations designed to disrupt the putative stem and to restore it with different nucleotides. Substitutions in either of the tetranucleotides abrogated VA RNA function in two independent PKR-based assays, demonstrating the importance of these sequences in vivo. Compensating mutants restored function, indicating that the two tetranucleotides pair in the cell, but all of the compensating mutants were less active than wild-type VA RNA. The effects of the mutations on RNA structure were probed by nuclease sensitivity analysis. Pronounced changes in two loops in the central domain correlated closely with the formation and disruption of the stem, suggesting that the tetranucleotide stem defines a critical element in the structure of the central domain through tertiary interactions with the two loops. A model for the central domain is presented that accommodates these findings and also accounts for the known sites of PKR interaction.

Keywords: adenovirus type 2 VA RNA; central domain; nuclease sensitivity analysis; tetranucleotide pairs; VA RNA–PKR interaction; structural model

INTRODUCTION

Adenovirus type 2 (Ad2) encodes two small (160 nt) polymerase III transcripts, VA RNA_I and VA RNA_{II} (see Mathews & Shenk, 1991, for review). The major species, VA RNA_I, accumulates to a high level in the cytoplasm of infected cells, where it plays an important role in regulating protein synthesis (Reichel et al., 1985; Schneider et al., 1985; Siekierka et al., 1985; Kitajewski et al., 1986; O'Malley et al., 1986). VA RNA_I binds to the cellular protein kinase PKR (also known as DAI, p68, P1-eIF2 kinase, etc.), the double-stranded (ds) RNA-activated inhibitor of translation, thereby preventing its activation (Schneider et al., 1985; O'Malley et al., 1986; Katze et al., 1987; Kostura & Mathews, 1989; Mellits et al., 1990b). In the absence of VA RNA_I, PKR is activated—presumably by dsRNA produced during viral infection (Maran & Mathews, 1988)—and phosphorylates the protein synthesis initiation factor eIF2 on its α subunit (Sen et al., 1978; Pathak et al., 1988; O'Malley et al., 1989). Phosphorylation of eIF2 leads to the inhibition of protein synthesis by imposing a block at the initiation step (Reichel et al., 1985; Schneider et al., 1985; Hershey, 1989). VA RNA_I also stimulates expression of transfected genes (Svensson & Akusjärvi, 1985, 1990; Kaufman & Murtha, 1987) through interaction with PKR (Akusjärvi et al., 1987; Kaufman et al., 1989).

PKR is an interferon-induced enzyme best known for its involvement in the host anti-viral response (reviewed in Hovanessian, 1989; Samuel, 1991). It has also been implicated in other regulatory processes, such as cellular differentiation (Judware & Petryshyn, 1991), inhibition of cell proliferation (Pestka et al., 1987; Chong et al., 1992), apoptosis (Lee & Esteban, 1994), and suppression of tumorigenesis (Koromilas et al., 1992; Meurs et al., 1993; Barber et al., 1995). The activity of this kinase is regulated by RNAs: whereas

Reprint requests to: Michael B. Mathews, Cold Spring Harbor Laboratory, P.O. Box 100, Cold Spring Harbor, New York 11724, USA.
[3]Present address: University of California, San Diego, Cancer Center, 9500 Gilman Drive, La Jolla, California 92093-0684, USA.

dsRNA activates it, small structured RNAs such as VA RNA inhibit its activation. Despite their opposite effects, these regulators appear to bind to the same site on the protein (Kostura & Mathews, 1989; Katze et al., 1991; Green & Mathews, 1992). Activation is accompanied by autophosphorylation and requires the presence of dsRNA that is perfectly duplexed for at least 30 bp, but there is no discernible dsRNA sequence dependence (Hunter et al., 1975; Minks et al., 1979; Manche et al., 1992). The precise requirements for inhibition have not been defined, yet it is clear that higher-order RNA structure is critical. For example, although VA RNA is highly structured, it lacks a continuous duplex stretch longer than 20 bp: its function is highly sensitive to changes in sequence and secondary structure. Furthermore, other structured single-stranded RNAs are reported to activate, rather than inhibit, the kinase (see, for example, Li & Petryshyn, 1991; Thomis & Samuel, 1993; Maitra et al., 1994).

Considerable effort has been expended to elucidate the structural elements of VA RNA and discover the mechanism whereby it blocks the activation of PKR. Several approaches have been used, beginning with computer-assisted RNA folding prediction, nuclease sensitivity analysis, and mutagenesis, in conjunction with functional and PKR binding assays conducted in vivo and in vitro (Mathews & Shenk, 1991; Mellits et al., 1992; Pe'ery et al., 1993; Clarke et al., 1994; Ghadge et al., 1994; Clarke & Mathews, 1995; Rahman et al., 1995). Further studies have employed phylogenetic comparison (Ma & Mathews, 1993, 1996), PKR protection, and footprinting techniques (Clarke & Mathews, 1995; D.A. Circle, O.D. Neel, P. Clarke, L. Manche, M.B. Mathews, & H.D. Robertson, in prep.). As a result, three structural features have been identified (Fig. 1A): the apical stem-loop, central domain, and terminal stem (Mellits & Mathews, 1988; Furtado et al., 1989). The apical stem is responsible for efficient binding to PKR, and a correctly formed central domain is required for VA RNA function (Furtado et al., 1989; Mellits et al., 1990a; Clarke et al., 1994; Ghadge et al., 1994). Both of these structures are partially protected by PKR against enzymic and chemical attack (Clarke & Mathews, 1995). The length and position of the paired region at the base of the apical stem, rather than its specific sequence, are important for VA RNA function. Disrup-

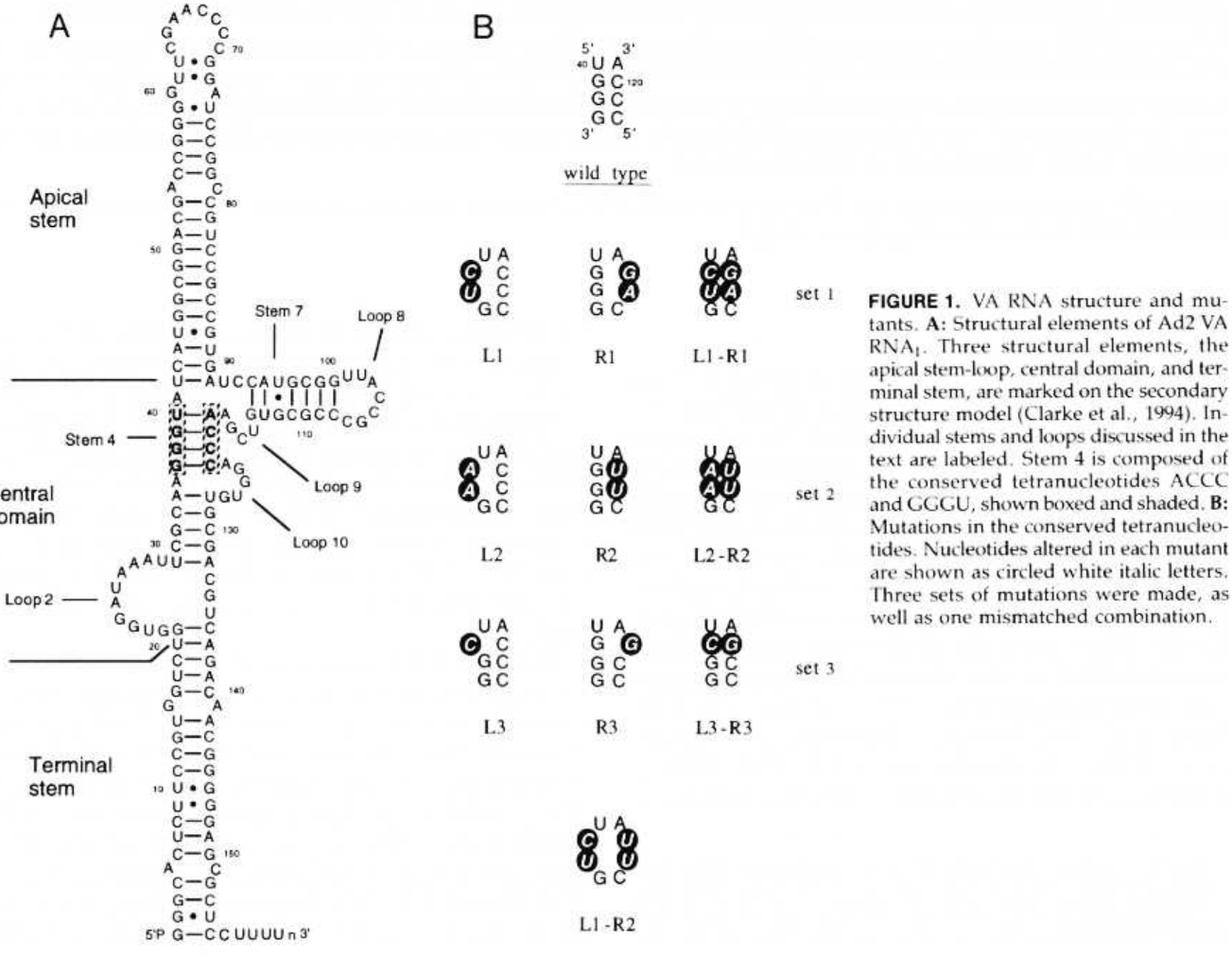

FIGURE 1. VA RNA structure and mutants. **A:** Structural elements of Ad2 VA RNA_I. Three structural elements, the apical stem-loop, central domain, and terminal stem, are marked on the secondary structure model (Clarke et al., 1994). Individual stems and loops discussed in the text are labeled. Stem 4 is composed of the conserved tetranucleotides ACCC and GGGU, shown boxed and shaded. **B:** Mutations in the conserved tetranucleotides. Nucleotides altered in each mutant are shown as circled white italic letters. Three sets of mutations were made, as well as one mismatched combination.

tion of this stem by mutations reduced the function of the RNA significantly, whereas a compensating mutation restored function to the wild-type level (Mellits et al., 1992). Because of its greater complexity, the structure of the central domain has been more difficult to elucidate through mutagenic studies (see Pe'ery et al., 1993, for example). Recently, the results of RNA structure probing (Clarke & Mathews, 1995), combined with the discovery of a pair of conserved, mutually complementary tetranucleotides, GGGU:ACCC (Ma & Mathews, 1993, 1996), suggested a defined secondary structure in the central domain (Fig. 1A). The short duplex formed by the pairing of the conserved tetranucleotides is a critical element of this structure.

Conservation of nucleotide sequences in evolution can follow from their involvement in base-specific interactions with protein ligands or from their participation in specific tertiary structures. The latter case is exemplified in tRNA, where most of the conserved and semiconserved bases are involved in tertiary interactions (Kim, 1978). Because no direct interactions between PKR and the base moieties of VA RNA have been detected (Clarke & Mathews, 1995), it seemed likely that the conserved nucleotides are responsible for maintenance of a correct central domain structure. To examine the role of these conserved nucleotides in the secondary and tertiary structure of the central domain and in the function of VA RNA, we have made three sets of mutants designed to disrupt and restore pairing of the tetranucleotides GGGU and ACCC. In each set, the disruption eliminated function and compensating mutations restored function, albeit not to the wild-type level. These results, together with data from nuclease sensitivity analysis of the mutant RNAs, support the view that the conserved nucleotides are paired and participate in a more complex higher-order structure. We infer a tertiary structure model for Ad2 VA RNA_I that involves interactions between two loops and the conserved stem in the central domain.

RESULTS

The central domain of Ad2 VA RNA_I plays an important role in blocking the activation of PKR. Although variable in sequence among adenovirus serotypes, the central domain contains two highly conserved tetranucleotides, GGGU and ACCC, that are potentially able to base pair with one another (Ma & Mathews, 1993) and occupy similar positions in nearly all other VA RNA species (Ma & Mathews, 1996). To assess the functional significance of these sequences and determine whether they indeed pair with one another to form stem 4, as shown in the model of Figure 1A, we constructed three sets of mutants, sets 1, 2, and 3. Each set consists of a mutant altered in the GGGU sequence (L1, L2, or L3), a corresponding mutant altered in the ACCC sequence (R1, R2, or R3), and a matching double mutant (L1-R1, L2-R2, or L3-R3). As diagrammed in Figure 1B, the double mutations were designed to restore base pairing that is disrupted by the individual L and R mutations, if indeed these sequences pair in the wild-type RNA molecule. In selecting these mutations, we used computer predictions of base pairing schemes to minimize the risk that the mutant sequences would form alternative structures by invading the wild-type structure. The consequences of the nine mutations were tested in two functional assays, and their effects on VA RNA structure were determined by nuclease sensitivity analysis. For comparison, two apical stem mutants (*dl*1 and A2dl2) were also tested, as well as a mismatched combination in the central domain (L1-R2).

Functional compensation

A priori, several possible outcomes could be envisioned for the effects of the central domain mutations on VA RNA function. In light of the model illustrated in Figure 1A, if both the sequences GGGU and ACCC are important for the proper folding or functioning of VA RNA_I, mutations in the L or R series would be expected to diminish the molecule's activity in functional tests. Furthermore, in the event that these sequences base pair with one another, the matching double mutants should display increased activity compared to the single mutants. On the other hand, if they do not base pair, the double mutations should be at least as deleterious as the single mutations. Finally, if the matching double mutants do indeed restore activity, indicative of base pairing between the two tetranucleotides, the degree of functional compensation would indicate whether the sequences GGGU and ACCC are specifically required, as suggested by their conservation, or whether their mutual complementarity is sufficient.

The two assays for VA RNA function that we employed to test this series of mutants are illustrated in Figures 2 and 3. The first assay employed cells infected with the adenovirus mutant *dl*331, which produces no VA RNA_I as a result of a deletion in its VA RNA_I gene. PKR is activated in the *dl*331-infected cells, and consequently protein synthesis is shut down during the late phase of infection relative to cells infected with wild-type virus (Thimmappaya et al., 1982; Kitajewski et al., 1986; O'Malley et al., 1986). Protein synthesis was rescued by transfecting the cells with a plasmid encoding wild-type VA RNA_I (Fig. 2A, compare lanes 1 and 2 with lanes 25 and 26). Mutant VA RNAs *dl*1 and A2dl2, which carry deletions in the apical stem but have an intact central domain, were also able to rescue translation in this assay (Fig. 2A, lanes 3–6), as found previously (Mellits & Mathews, 1988), in keeping with the conclusion that the apical stem is less critical for VA RNA function than the central domain (Mellits et al., 1990a).

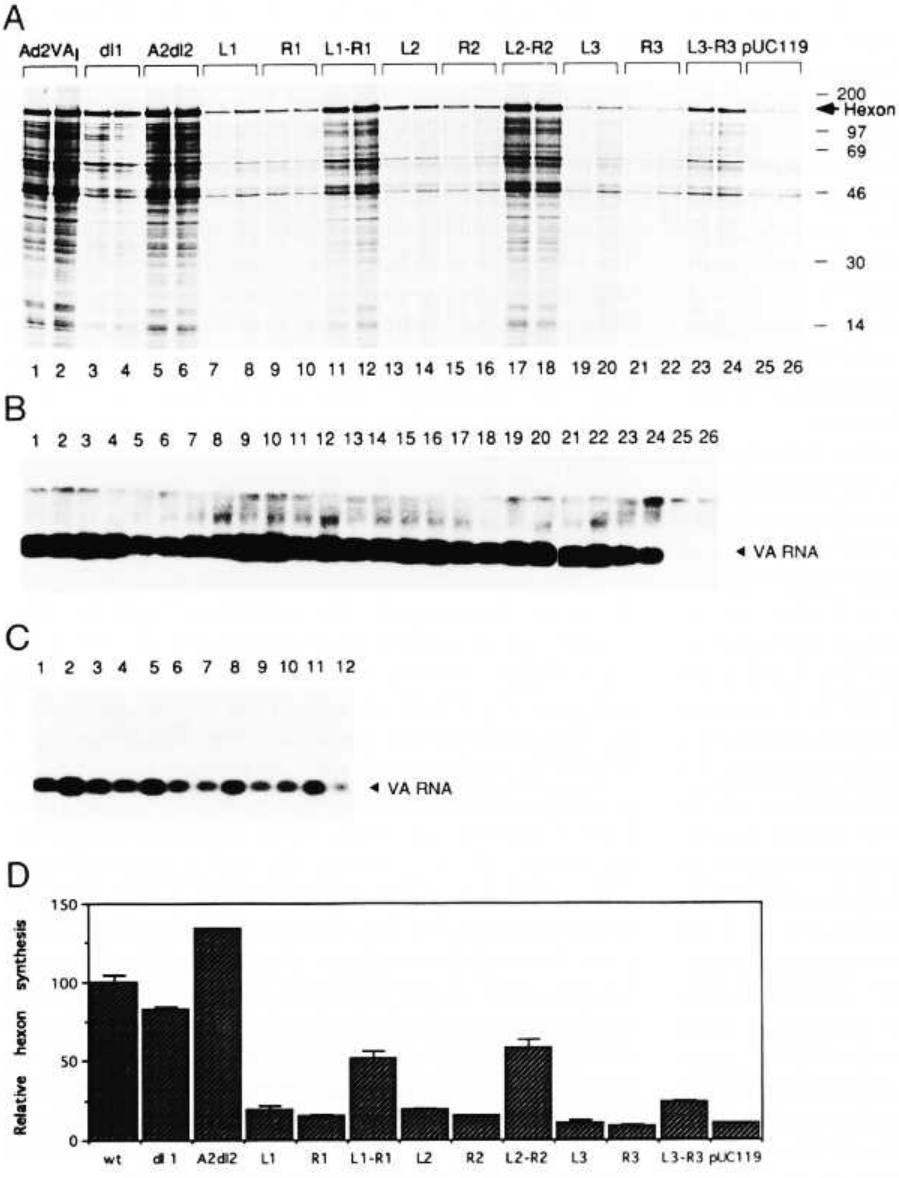

FIGURE 2. Translation rescue assay. Duplicate 293 cell cultures were transfected with plasmids encoding the wild-type Ad2 VA RNA$_I$ gene, the mutants shown, or the vector pUC119, and then were infected with the mutant adenovirus *dl*331. **A:** The ability of the VA RNAs to rescue translation was determined by labeling with [^{35}S]methionine and SDS-PAGE. Positions of hexon and molecular weight standards (in kDa) are marked. **B:** The accumulation of VA RNAs, run in duplicate in the same order as in A, was monitored by northern blot assay. The VA RNA band is marked. **C:** As a control for RNA transfer and detection, 22 ng of each VA RNA species, synthesized by T7 RNA polymerase and purified by gel filtration, was loaded on a separate gel and probed in parallel to the gel of B. RNAs were run in the same order as in A. Mutations in the L and L-R series cause reduced signal intensity due to imperfect pairing with the probe. **D:** Quantitation of hexon labeled in A, an index of late viral protein synthesis. Scanned values were averaged and normalized to the wild-type VA RNA$_I$ (wt) control value. Error bars denote deviations from the average of two duplicate samples.

None of the mutants in the central domain tetranucleotides rescued protein synthesis to the same extent as wild-type VA RNA, but, within each set, the double mutant was more effective than either of the single mutants (Fig. 2A, lanes 7–24). To quantify this observation, the radioactivity in the most prominent viral protein, hexon (marked with an arrow on Fig. 2A), was measured using a radiographic image analyzer. The data confirm that the single mutants were essentially inactive and that the activity of the double mutants greatly exceeded that of the corresponding single mutants, but in no case did it approach the activity of wild-type VA RNA$_I$ (Fig. 2D). The mismatched double mutation L1-R2 was as deleterious as the corresponding single mutations L1 and R2 from which it was derived (data not shown). Northern blot analysis verified that all of the VA RNAs were expressed to comparable levels (Fig. 2B,C).

These results indicated that the two tetranucleotides are important for VA RNA function and suggested that their significance is due, at least in part, to their ability to pair with one another. To substantiate this conclusion, we employed a transient expression assay in uninfected cells. In cells transfected with a CAT expression vector, the expression of CAT protein is limited by PKR activation, and can be stimulated by cotransfection of a plasmid carrying the VA RNA$_I$ gene (Akusjärvi et al., 1987; Davies et al., 1989; Svensson & Akusjärvi, 1990). We examined CAT protein synthesis by immunoprecipitation with antibody (Fig. 3A). The results, together with those obtained by assaying CAT enzyme activity, were quantified and are represented

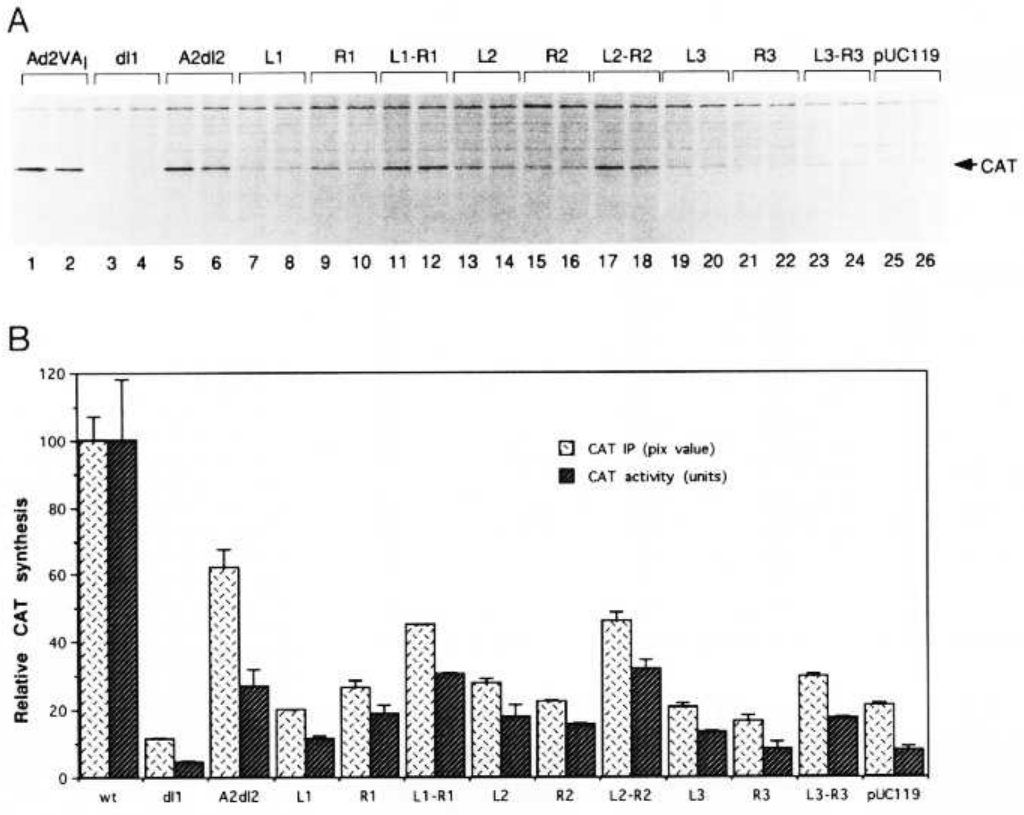

FIGURE 3. CAT expression enhancement assay. Effect of the cotransfected VA RNA plasmids indicated, or the vector pUC119, on CAT expression from pβCAT-6.5 was measured by immunoprecipitation (IP) of [^{35}S]methionine-labeled CAT and by CAT enzyme assays. **A:** Immunoprecipitated CAT was resolved in a 15% polyacrylamide-SDS gel. The position of CAT is marked with an arrow. **B:** CAT protein in A was quantified and averaged results are depicted (speckled bars) together with the average of CAT enzyme activities measured in parallel (striped bars). Values were normalized to the wild-type VA RNA$_I$ (wt) control value. Error bars denote deviations from the average of two duplicate samples.

in Figure 3B. All the VA RNAs were expressed to comparable extents (not shown). Both wild-type Ad2 VA RNA$_I$ and the apical stem mutant A2dl2 increased CAT expression, but *dl*1, the other apical stem mutant, did not. The discrepant behavior of *dl*1 has been noted before (see the Discussion). None of the tetranucleotide mutants was as effective as wild-type VA RNA$_I$, but the three matched double mutants were more active than the corresponding single mutants, which were almost devoid of activity. These results demonstrate functional compensation. As in the *dl*331 assay, L3-R3 was the least active of the three double mutants despite the fact that it contains only one altered base pair, whereas L1-R1 and L2-R2 contain two altered base pairs. Again, the mismatched combination mutant L1-R2 was inactive (data not shown), supporting the conclusion that compensation requires sequence complementarity.

Secondary structure analysis

These results provide strong evidence that the two tetranucleotide sequences base pair with one another in the wild-type RNA molecule. Furthermore, the observation that the base compensation mutations gave only partial restoration of function implies that the tetranucleotide stem might be involved in higher-order structure. To determine the impact of the mutations on RNA structure, the transcripts were examined using the nuclease sensitivity technique. Each RNA was labeled at its 5′ or 3′ end, then subjected to mild digestion with a battery of nucleases of differing specificity to detect accessible sites. Digestion products were resolved by electrophoresis in sequencing gels as shown in Figure 4 for the 3′ end-labeled RNAs. Wild-type VA RNA$_I$ and the two apical stem mutants, *dl*1 and A2dl2, were examined in parallel. The sites and intensities of attack by single-strand-specific and structure-specific nucleases are summarized in Figures 5 and 6. The wild-type VA RNA$_I$ cleavage pattern is shown in full (Fig. 5A), but for the mutants, only the relevant part of the model is shown because, in all cases, the effects of the mutations on nuclease sensitivity were confined to the domain in which the mutations were located. Thus, the nuclease sensitivity data imply that the apical stem and central domain behave as relatively autonomous regions of the VA RNA molecule.

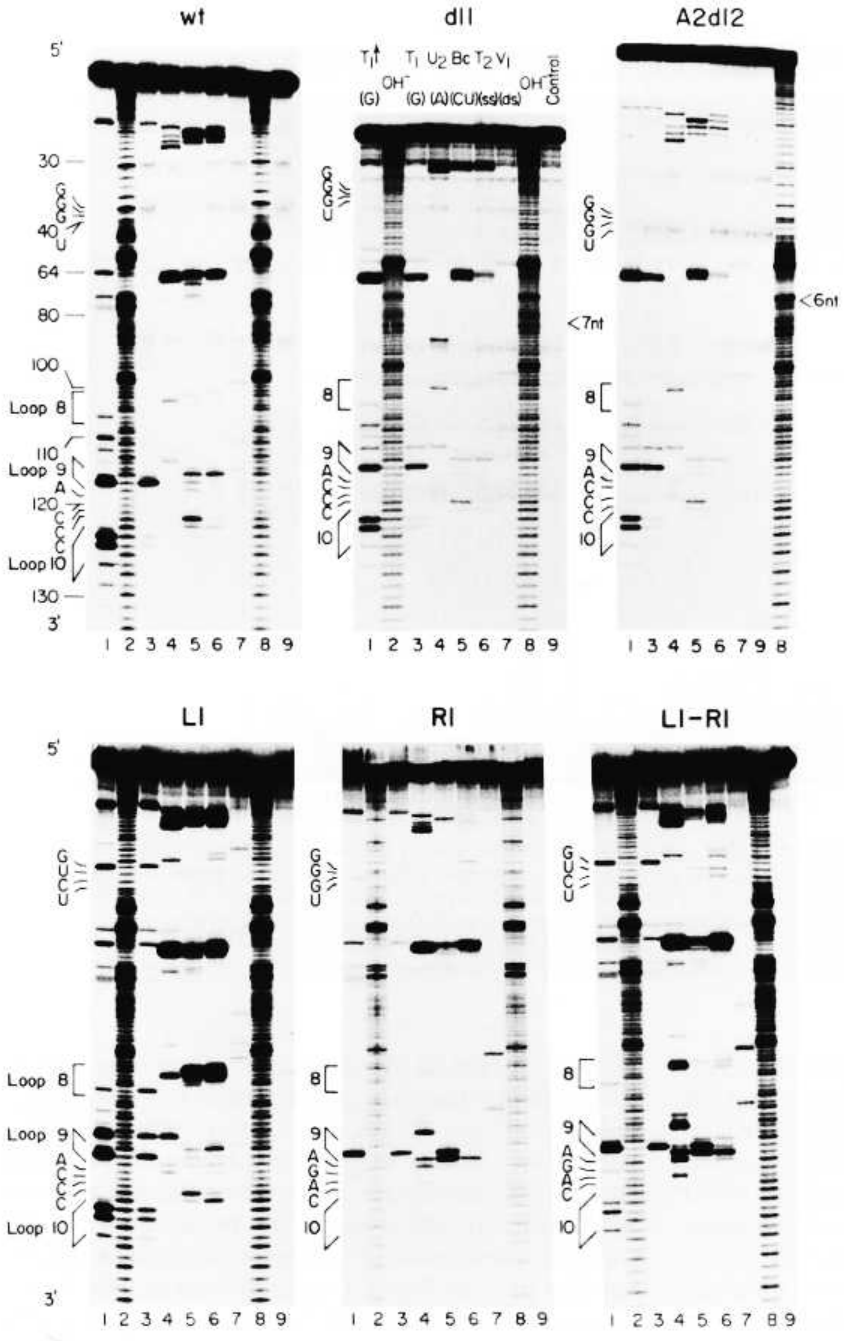

FIGURE 4. Nuclease sensitivity analysis. Mutant and wild-type VA RNAs were labeled at the 3' end and partially digested with the nucleases indicated. Resulting RNA fragments were separated in 8% polyacrylamide-urea gels. RNA in lanes 3–7 was digested with RNases T_1, U_2, Bc, T_2, or V_1, respectively. RNA in lane 1 was digested with RNase T_1 at 68 °C to disrupt VA RNA secondary structures, allowing digestion of most G residues and providing markers. RNA in lanes 2 and 8 was digested with alkali to cleave at all possible nucleotide positions. Lane 9 contains a negative control, with water in place of nucleases. Nucleotide positions from the 5' end are marked on the wild-type (wt) VA RNA gel. Positions of the tetranucleotides and of loops 8, 9, and 10 are marked on the side of each gel. Some nucleotides in the central domain were cut anomalously. These include G114, which is not cut by RNase T_1, but is cut by RNase U_2 in wild-type VA RNA and the R series mutants, and is cut by both enzymes in the L series mutants; A123, which is not cut by RNase U_2, but is cut by RNases Bc and T_2 in wild-type, L1, and L2, and by T_2 in L3-R3; G117 and A118, which are also cut by RNases Bc and T_2, as well as by RNase T_1 and U_2, respectively. (*Figure continues on facing page.*)

The apical stem mutants gave cleavage patterns identical to that of wild-type VA RNA (Fig. 5A), except at the top of the apical stem-loop. As reported previously (Mellits et al., 1992), base pairing in this region rearranges slightly because of the deletions, such that the apical loop contains nt 61–66 in both *dl*1 and A2dl2 (Fig. 5C,D) instead of nt 63–70, as in the wild-type structure drawn in Figure 5A. Mild digestion at nt 72–78 suggests that at least a fraction of the wild-type RNA molecules also exists in a conformation similar to that of the two apical stem mutants, with nt 61–66 forming the apical loop and nt 73–79 extruded in a bulge (Fig. 5B). Unlike *dl*1 and A2dl2, however, the wild-type molecule exhibits strong cleavages at A65 and A66, indicating that a large fraction of it is present in the conformation shown in Figure 5A, with the apical loop located between nt 63 and 70 and with no bulge. Possibly the wild-type apical stem is in equilibrium between the isomers shown in Figure 5A and B.

In contrast to the limited scope of the cleavages elicited by these apical stem deletions, the substitutions in the central domain tetranucleotide stem resulted in numerous changes at the sites of mutation and throughout the central domain (Fig. 4), reflecting the complex

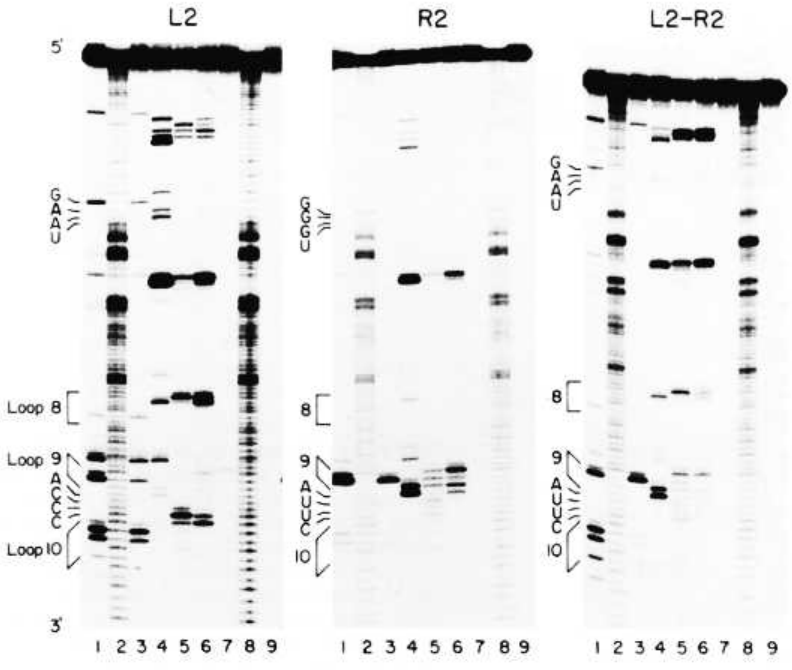

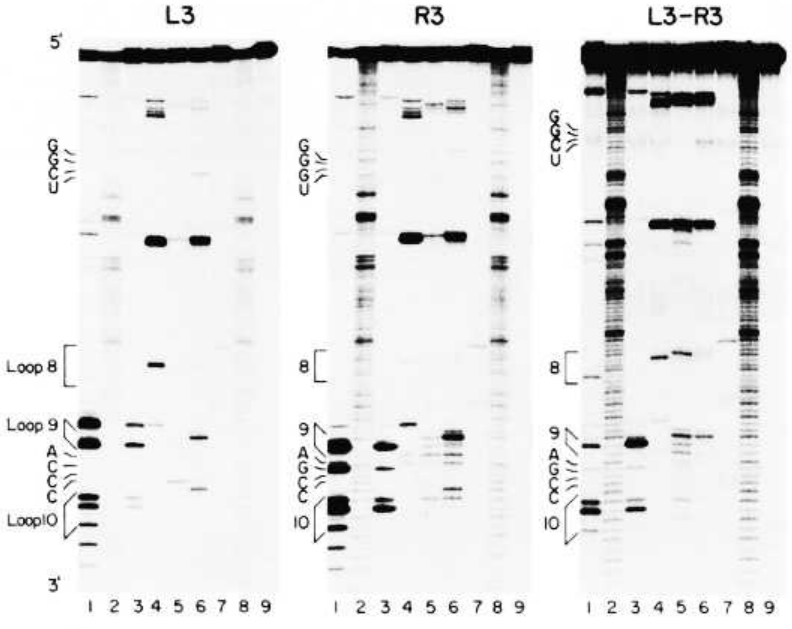

FIGURE 4 (*continued*)

tertiary structure of this region. Despite these perturbations, there was no evidence of drastic rearrangements in the secondary structure: for example, stem 7, the longest stem in the central domain, was not disrupted by the mutations. Therefore, we have illustrated the digestion patterns for each mutant RNA by superimposing the cleavage sites on the secondary structure model for the wild-type central domain (Fig. 6). Several general conclusions can be drawn that are exemplified most clearly by mutants in sets 1 and 2, whereas the changes in set 3 are more subtle.

All six of the single mutations (L1, L2, L3, R1, R2, and R3) caused increased sensitivity to single-strand-specific nucleases at the site of mutation and, in some cases, also at adjacent sites. Less predictably, increased cleavage on the opposite side of stem 4 was not generally observed. Furthermore, in the double mutants (L1-R1, L2-R2, and L3-R3), the sensitivity of stem 4 to single-strand-specific nucleases often remained high despite the compensating nature of the mutations and the partial restoration of function documented above. These observations do not, on the face of it, confirm the proposed stem 4 pairing. Changes elsewhere in the central domain provide indirect support for the stem 4 pairing scheme, however. The most pronounced of these distant changes were in loop 8 and loop 10, which

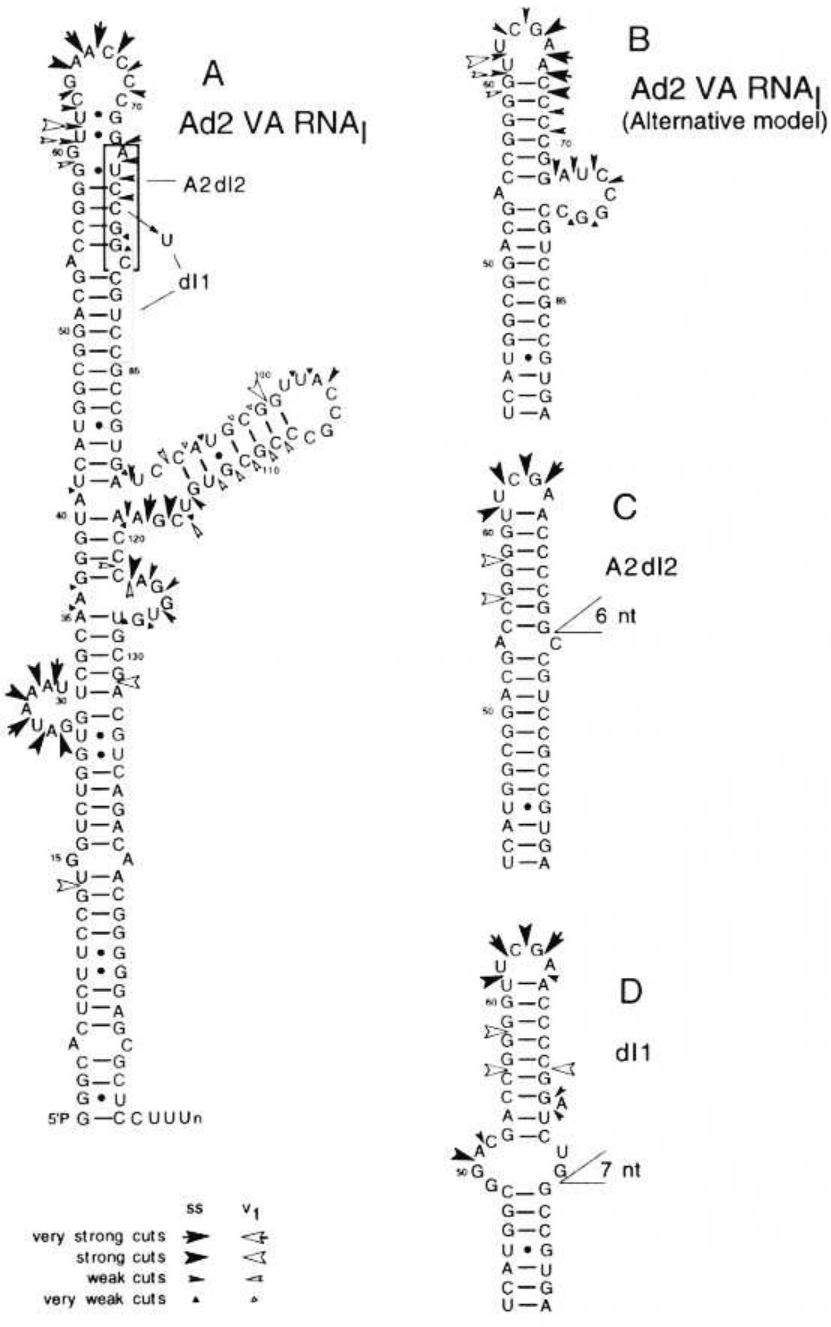

FIGURE 5. Cleavage sites in wild-type Ad2 VA RNA$_I$ and apical stem mutants. **A:** Nuclease sensitivity of the entire wild-type molecule. Filled arrows, sites of cleavage by the single-strand-specific (ss) nucleases RNase T_1, T_2, U_2, or Bc; open arrows, sites of cleavage by nuclease V_1; large arrows, very strong cleavages; large arrow heads, strong cleavages; small arrows, weak cleavages; small triangles, very weak cleavages. The bases deleted (boxes) and substituted (C76 → U)in A2dl2 and *dl*1 are also indicated. **B:** An alternative conformation for the apical stem of wild-type VA RNA. **C,D:** Apical stem-loop structure of mutants A2dl2 and *dl*1, respectively. The central domain and terminal stem region of these two mutants gave cleavage patterns identical to that of wild-type VA RNA. Sites of the A2dl2 and *dl*1 mutations are marked in A.

responded in a coordinated fashion to mutations in stem 4 (Figs. 4, 6). The sensitivity of nucleotides in both of these loops to single-strand-specific nucleases was increased by mutations in the L series, and decreased by mutations in the R series. In the double mutants (L-R series), nucleotides in loop 8 and 10 displayed a sensitivity intermediate between that of the L and R mutants, resembling quite closely the wild-type pattern and intensity of cleavage. Changes in nuclease sensitivity in other parts of the central domain (stem 3, stem 7, and loop 9), both with single-strand-specific and structure-specific enzymes, were relatively minor, implying that the concerted changes in loops 8 and 10 are probably attributable to tertiary structure alterations consequent upon the mutations in stem 4. Presumably the minor changes visible in stem 7, loop 9, and elsewhere are also contingent on the conformational changes due to disruption of stem 4 (see below).

Central domain structure

Several observations suggested that stem 4 and other parts of the central domain are mutually interdependent elements of tertiary structure. First, compared to other loops in the molecule (such as loop 2 and the apical loop), ostensibly single-stranded nucleotides in

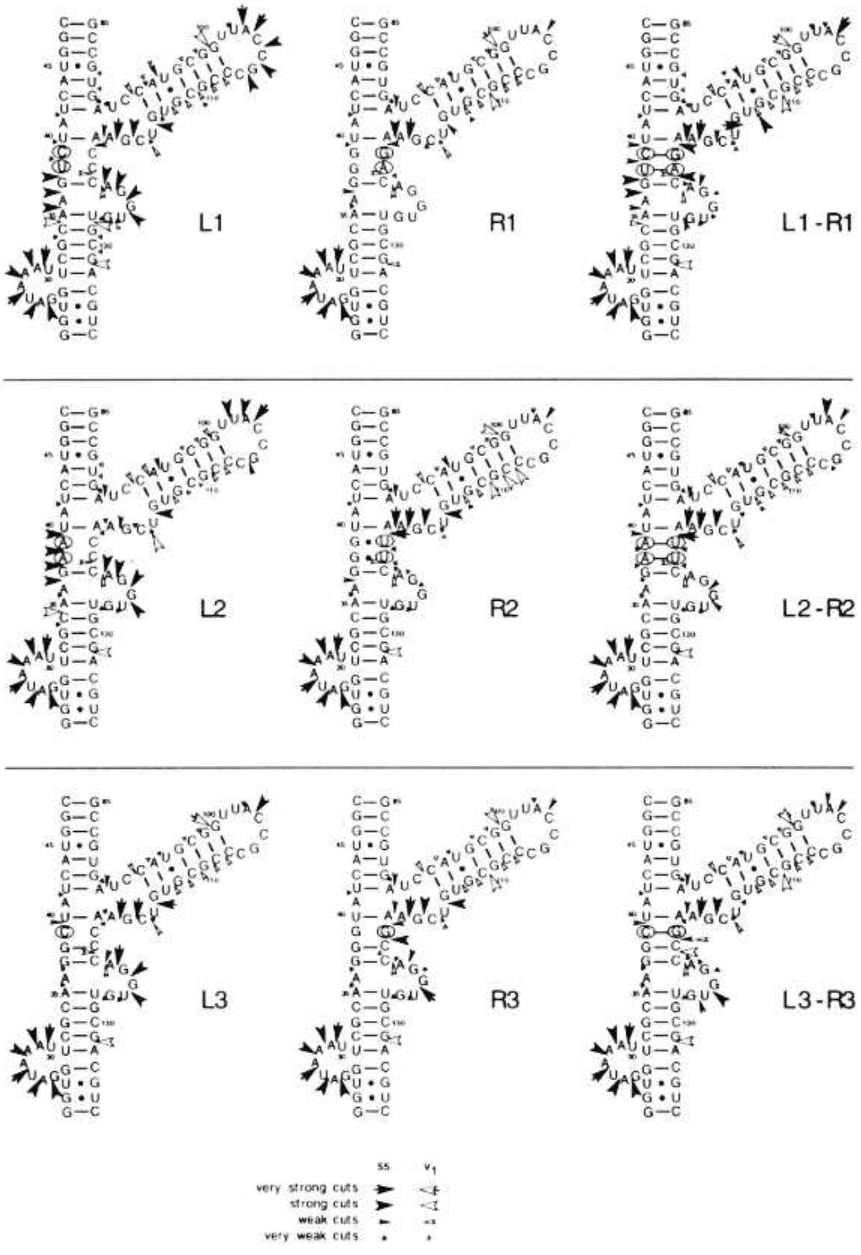

FIGURE 6. Cleavage sites in the central domain of the stem 4 mutants. Nuclease sensitivity data from each of the mutants were superimposed on the wild-type VA RNA central domain model, using the same convention as in Figure 5. Mutant nucleotides are circled, and base pairing has been removed if the mutation disrupts base pairing. The apical stem-loop and terminal stem region of these mutants gave cleavage pattern identical to that of wild-type VA RNA_1.

loops 8 and 10 are relatively insensitive to digestion with single-strand-specific enzymes (Figs. 4, 5A). Second, as mentioned above, their sensitivity to single-strand-specific nucleases is increased by mutations in the GGGU sequence, reduced by mutations in the ACCC sequence, and returned toward normal in the compensating mutants. This coupling suggests that pairing of loops 8 and 10 or steric hindrance due to a stem 4-dependent tertiary structure may be involved. Third, there are anomalous cleavages in the central domain that can signify the existence of tertiary structure (Puglisi et al., 1988). These include examples of aberrant specificity (as listed in Fig. 4) and nucleotides that are recognized by nuclease V_1, as well as single-strand-specific enzymes (such as U115 in loop 9). Finally, cleavage in the central domain (including stem 4, loop 8, and loop 10) by single-strand-specific nucleases is suppressed when digestion is conducted in the presence of Mg^{2+} (Clarke & Mathews, 1995, and data not shown), implying the existence of a Mg^{2+}-dependent higher-order structure in the central domain.

Based on these observations, we generated a three-dimensional model in which loops 8 and 10 are spatially adjacent and form a pseudoknot as a result of the folding and twisting of stem 7 (Fig. 7). The existence of stem 4 is essential for the approximation of loops 8 and 10, and it probably also strengthens the structure through base-specific interactions with loop 8. Loop 8 contains the sequence ACC (nt 103–105), which is capable of pairing with the sequence GGU (nt 124–126)

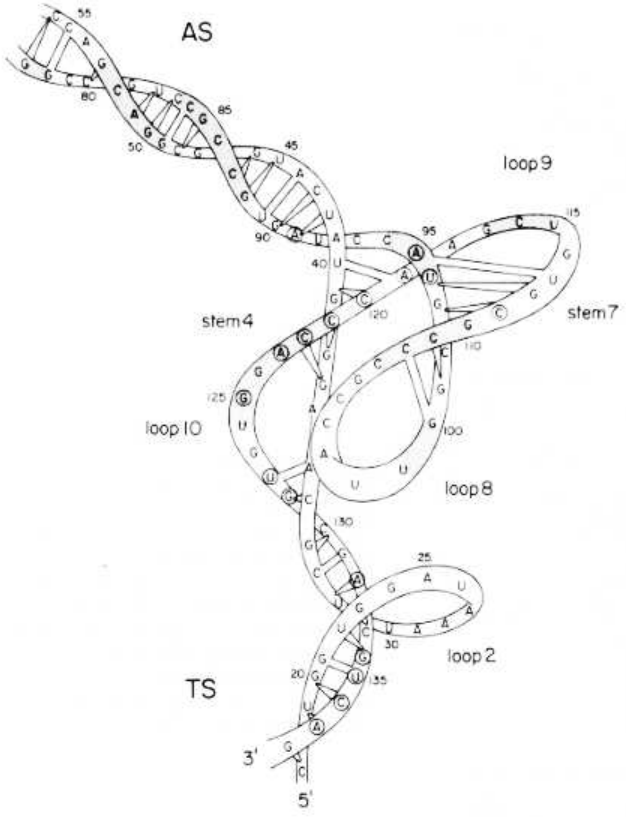

FIGURE 7. Model showing possible tertiary structure in the central domain of Ad2 VA RNA_I. Watson–Crick base pairing is indicated. Nucleotides are marked along the backbone (drawn from a wire model) and subregions are identified. Stippling indicates nucleotides protected by PKR (Clarke & Mathews, 1995). Point mutations at the circled nucleotides are deleterious to function (Rahman et al., 1995). AS, apical stem; TS, terminal stem.

in loop 10 to form a pseudoknot; such pairing could account for the relative resistance of these nucleotides to cleavage in the wild-type molecule. Analogous pairings are possible in other VA RNAs (Ma & Mathews, 1996). Furthermore, the nucleotides GCC (nt 106–108), at the 3′ end of loop 8, are positioned close to stem 4 and might be engaged in tertiary interactions with the duplexed nucleotides of stem 4. Nucleotides that interact with PKR (Clarke & Mathews, 1995) occupy a region on one surface of the model (shaded, Fig. 7).

Nuclease sensitivity analysis of the three sets of mutant RNAs supports many features of the model. First, most of the alterations in nuclease sensitivity caused by the mutations are increases or decreases in the intensity of cleavage at nucleotides that are sensitive to nucleases in wild-type VA RNA. In other words, there are few new cleavage sites, consistent with the view that the general structure of VA RNA is quite robust and preserved in the mutants. Second, the changes in cleavage intensity are usually more profound on the 3′ (right) side of VA RNA (loops 8, 9, and 10) than on its 5′ (left) side, irrespective of the mutation site. This is in keeping with the overall features of the model because the 3′ side is exposed at the surface of the molecule. Third, many of the detailed changes in sensitivity in loops 8 and 10, and to some extent in loop 9, brought about by mutations in stem 4, indicate that these elements are mutually bound and in close proximity to one another. For example, the increased cleavage of both loops 8 and 10 that accompanies disruption of stem 4 in mutants L1 and L2 can be explained by the tertiary structure opening up and causing the two loops to separate.

Such structural deformations presumably lead to a functionally inadequate central domain. In the compensating mutants L1-R1 and L2-R2, the wild-type structure is largely, but not completely restored, and function returns concomitantly. Evidently, the pairing in stem 4 is not fully reconstituted, possibly because the nucleotide changes alter tertiary interactions with loop 8 nucleotides that are needed to stabilize the structure. The set 3 mutants present an apparent anomaly in that their function is severely compromised, yet they display the least disturbance of structure. Mutants L3 and R3 exhibit cleavages in loops 8 and 10 that are similar in nature to those observed in sets 1 and 2, although they are less extreme in degree. Possibly these mutations do not disrupt stem 4 completely because only one nucleotide is altered. However, the single nucleotide mutations may disrupt tertiary interactions that are required for function, and different interactions may be formed instead. For example, the two remaining G:C pairs (nt 37:122 and 38:121) in the mutated stem 4 of R3 and L3 are capable of interacting with C104 and C105 in loop 8 through base triples. L3-R3 appears to form a structure somewhat different from that of L1-R1 and L2-R2, as signified by increased cleavages in loop 10 (at G125 and U126). Possibly the GCC sequence in loop 8 interacts with stem 4, explaining why L3-R3 is slightly less active than the other two compensating mutants.

DISCUSSION

Phylogenetic analysis of the VA RNAs of human adenoviruses indicated that two mutually complementary tetranucleotides, GGGU and ACCC, in the central domain are nearly invariant (Ma & Mathews, 1993, 1996). In only two viruses is one of the sequences changed, and in these cases ACCC is replaced by ACCU, which is still able to pair with GGGU. This conservation in itself suggests that the tetranucleotides play an important role and probably pair with one another. The nearly absolute sequence conservation might reflect constraints imposed by higher-order RNA structure or by RNA–protein interactions, but no base-specific interactions with PKR have been observed (Clarke & Mathews, 1995). To examine the significance of the tetranucleotides, we made three sets of mutations to

disrupt and restore the potential base pairing, and determined their effects on structure and function.

In two independent assays, both of which depend on the VA RNA–PKR interaction, mutation of the tetranucleotides abrogated VA RNA function in vivo, whereas compensating changes partially restored function. Similar behavior was observed for one set of mutants in a PKR binding assay (Clarke & Mathews, 1995). These results imply that the two tetranucleotides pair and form a stem. However, the partial nature of the compensation indicates that pairing is necessary but not sufficient for function, a finding that is consistent with the very high degree of sequence conservation in the tetranucleotides. To understand the molecular basis of the functional compensation, we probed the structure of the mutant RNAs with nucleases. Although nuclease sensitivity changes provided little direct support for the pairing of the GGGU and ACCC tetranucleotides, they suggested the existence of this pairing indirectly, through coordinated changes of nuclease sensitivity within the central domain. These findings led to a model in which the tetranucleotides contribute to the structure of the central domain not only by forming a double-stranded stem, but also by interacting with nucleotides in adjacent loops.

Pairing of the conserved tetranucleotides

The fact that single mutations in the tetranucleotides abolished VA RNA function and compensating mutants restored function to a substantial extent constitutes strong evidence for the pairing of the GGGU and ACCC sequences. This conclusion is supported by the coordinated changes in sensitivity of loops 8 and 10 in response to mutations in stem 4. However, in the central domain, the relationship of the two regions is not as straightforward as in the simple two-strand interaction in the apical stem (Mellits et al., 1992). Mutations in either one of the two tetranucleotides resulted in increased digestion at the site of mutation, but did not greatly increase the sensitivity of the opposing tetranucleotides to single-strand-specific nucleases, nor did introduction of a compensating mutation greatly reduce the nuclease sensitivity of the first mutant sequence. Although unexpected, these findings are explicable in terms of the network of interactions that frames the central domain (see below).

Nevertheless, we also considered a number of additional factors that might contribute to the difficulty of detecting the reformation of stem 4 by probing the mutant RNAs. One concern was that the mutant nucleotides might engage in alternative base pairing schemes that compete with the wild-type stem structure. However, it is unlikely that all of the mutants would have formed stable alternative structures, especially because attention was paid to this contingency in designing the mutants; furthermore, little evidence for the formation of other structures was obtained by nuclease sensitivity analysis. A second possibility was that the duplexes formed by the compensating mutations might be intrinsically less stable than the wild-type GGGU:ACCC pair. By calculation, this is indeed the case for L1-R1 and L2-R2, which have theoretical free energies of −6.1 and −4.1 kcal/mol and could therefore be expected to be less stable than the wild-type tetranucleotide pair (−7.9 kcal/mol). However, this parameter cannot account for the properties of L3-R3, which has a calculated free energy very similar to that of the wild-type pair (−8.0 kcal/mol). A third possibility, which is harder to evaluate, is that the nuclease sensitivity analysis conducted might not fully represent the structure of the RNA in vivo. Even though the ionic conditions used were close to physiological (except for RNase U_2, which requires acidic pH), RNA structure is influenced by RNA-binding proteins and other factors that are difficult to duplicate in vitro. In this connection, we note that PKR is able to enforce a native conformation upon the central domain in the absence of Mg^{2+} (Clarke & Mathews, 1995); by analogy, the enzyme may be able to compensate, at least partially, for suboptimal pairing in stem 4. In other words, the stem 4 structures of the double mutants may pair more effectively in the presence of PKR than in its absence. Although the data do not exclude the possibility that the tetranucleotide pair GGGU:ACCC is important per se, for example, because it is recognized by PKR or other proteins in the cell, they clearly establish it as a key element in the VA RNA tertiary structure.

A complex structure in the central domain

In the central domain model, illustrated in Figure 7, stem 4 and other parts of the central domain are mutually interdependent elements of an intricate tertiary structure. The 5′ strand forms one side of a more or less continuous duplex axis, whereas the serpentine 3′ strand adopts an ampersand-like conformation (viewed upside down from the representation in Fig. 7). In so doing, the 3′ strand makes a number of turns and contacts that are reflected in its nuclease sensitivity pattern. For example, nt U115 is cut by nuclease V_1 as well as by RNases T_2 and Bc, whereas its neighbors are only recognized by single-strand-specific nucleases. Anomalous behavior is also displayed by nt A95, which is expected to pair with U113, but is weakly cut by RNase U_2. These two nucleotides are located at the twist junction between stem 7 and the main axis of VA RNA, and their unusual sensitivity to nucleases may be due to the kink that results from the bending or to a base triple with U115, as in HIV-1 TAR RNA (Puglisi et al., 1992). Triple hydrogen bonds are found in tRNAs as part of their L-shaped tertiary structure (Kim, 1978). It is notable that A95 and U96 were identified as

important nucleotides by mutagenesis (Rahman et al., 1995).

In the three-dimensional model, loop 8 is in intimate contact with loop 10, and is also brought close to loop 2. This juxtaposition offers an explanation for observations made with mutant *ls*3a (Pe'ery et al., 1993). Substitution of nt 103–109 in loop 8 reduced VA RNA function and concomitantly reduced nuclease sensitivity in loop 2. Because these loops are adjacent in the model of Figure 7, it is possible that the substituted nucleotides interact with nucleotides in loop 2. Consistent with this interpretation, a point mutation at A132, near loop 2, caused widespread alterations in VA RNA structure and also affected function severely (Rahman et al., 1995).

Strikingly, the regions of VA RNA that are protected by PKR from attack by nucleases and chemicals, which are scattered through the central domain in the secondary structure representation (Clarke & Mathews, 1995), lie on the same surface in the three-dimensional model (Fig. 7). As in the U1 RNA-U1A protein complex (Jessen et al., 1991), PKR appears to cover one face of VA RNA. The protected regions include one helical turn at the base of the apical stem, part of both sides of stem 7, which are on one surface, loop 9, the two 3′-terminal residues of the ACCC sequence, and loop 10. Several of the same nucleotides were shown to be important for VA RNA function in vitro in a study of point mutations covering the 3′ side of the central domain (Rahman et al., 1995). Mutation of the ACCC sequence, and of other nucleotides shown circled in Figure 7, reduced the ability of VA RNA to block PKR activation, whereas mutation of the remaining nucleotides between nt 88 and 137 had little or no effect. Few changes in nuclease sensitivity were observed (Rahman et al., 1995), but the significance of this finding is unclear because it appears that the RNA structure was probed in the absence of Mg^{2+}, which is known to play a key role in central domain folding (Clarke & Mathews, 1995).

Contribution of the stems

The proposed three-dimensional structure (Fig. 7) emphasizes the role of the stems in forming an almost continuous axis for the VA RNA molecule. The lower part of the apical stem is important for VA RNA function (Mellits et al., 1992): its duplex nature is probably necessary to allow the folding of stem 7 toward stem 4. Stem 4 is also important for function: in this case, both structure and sequence are critical. This short stem appears to be responsible for the maintenance of a compact tertiary structure in which loop 8, loop 10, and stem 4 interact in concert, probably with the involvement of Mg^{2+}. The details of the interactions are not yet known, but possibly the apical stem and stem 4 act as clamps, cooperating to facilitate the twisting of the central domain that enables the pseudoknot to form. Mutations that disrupt pairing in stem 3 and at the top of the terminal stem are also deleterious (Furtado et al., 1989; Ghadge et al., 1994; Rahman et al., 1995), suggesting that these stems also contribute to VA RNA function, whereas mutations that perfect the base pairing were permissible (Ghadge et al., 1994).

In the apical stem, at least eight base pairs proximal to the central domain are needed for efficient binding to PKR in vitro and for function in vivo, although sequence changes are tolerated (Mellits & Mathews, 1988; Mellits et al., 1990a, 1992; Clarke et al., 1994; Ghadge et al., 1994). On the other hand, the distal part of the apical stem seems less critical. Mutations A2dl2 and *dl*1 have no impact on the nuclease sensitivity in the central domain, and stem 4 mutations do not affect the apical stem, suggesting that these regions are, to some extent, independent of one another. It may not be coincidental that the apical stem of many VA RNAs has a discontinuity about 6–7 bp above the central domain, separating a stably paired region from a region that is variable in size and in duplex character (Ma & Mathews, 1996). In Ad2 VA RNA_I, there is evidence for more than one wild-type structure above this point (Fig. 6B). Possibly this distal region subserves an additional function, related to the anomalous behavior of *dl*1 in a PKR binding assay (Mellits et al., 1990a; Clarke et al., 1994) and in the functional assays reported here. Both the *dl*331 rescue and CAT expression assays reflect the regulation of PKR activation by VA RNA, but a secondary effect on mRNA stability has been reported in cotransfection (Strijker et al., 1989; Svensson & Akusjärvi, 1990). This action could be important in the CAT expression assays and it might require a structure in the distal part of the apical stem that is present in wild-type VA RNA and A2dl2, but not in *dl*1. Another possibility is that a viral product that is present in *dl*331-infected cells, but not in uninfected cells, is required for *dl*1 function: VA RNA_{II} has been considered as a candidate in this regard, but cotransfection of the VA RNA_{II} gene failed to cooperate with *dl*1 in CAT expression enhancement assays (data not shown). It remains possible that another viral product in *dl*331 makes *dl*1 functional in the cell, possibly by altering its apical stem structure.

Inhibition of PKR

The mutational study of the conserved tetranucleotides has yielded insights into the tertiary structure of the central domain. This domain is essential for VA RNA function and, together with the base of the apical stem, constitutes the binding site for PKR. The only known function for VA RNA is to block PKR activation, which is accomplished by binding to the enzyme's RNA binding domain. All attempts to date to distinguish the VA RNA binding site from the site for dsRNA binding have been unsuccessful (Green & Mathews, 1992;

McCormack et al., 1992; Green et al., 1995). These observations pose a question: what is the purpose of the elaborate central domain structure?

This question is especially pointed in light of the fact that perfectly duplexed dsRNA molecules of a size that are too short to activate PKR (i.e., <30 bp) are also able to bind to the enzyme and block its activation (Minks et al., 1979; Manche et al., 1992). Furthermore, VA RNA itself contains two stems in this size range, which could fulfill the inhibitory function. Mutants that are disrupted in the central domain but maintain intact apical and terminal stems retain the ability to bind PKR and inhibit its activation in vitro. The concentrations required for inhibition by such mutant VA RNAs are higher than for wild-type VA RNA_I, however, and are comparable to the concentration required for inhibition by dsRNA of 23 bp (Manche et al., 1992; Mellits et al., 1992; Pe'ery et al., 1993; Clarke et al., 1994; Ghadge et al., 1994). Careful examination of the kinetics of inhibition implies that short duplexes inhibit by simple competition, whereas the central domain interacts with the enzyme in such a way as to specifically prevent its activation even at low VA RNA concentration. Presumably, the role of VA RNA cannot be subserved by a simple duplex or hairpin molecule because it would be unstable in the cell or toxic at the relatively high concentration required. The special structure of the central domain may make VA RNA very compact and stable, protecting it from cellular enzymes that could modify, degrade, or unwind it.

In addition to its role in inhibiting PKR activation, the central domain contributes to PKR binding (Ghadge et al., 1991; Clarke et al., 1994). These properties are closely linked, but the behavior of some mutants suggests that they may be separable (Pe'ery et al., 1993; Clarke et al., 1994). If they are separable, a mechanism could be envisaged in which interactions of the central domain with PKR positively obstruct the enzyme's function, perhaps by masking some functional groups: in this case, it should be possible to find PKR mutants that affect dsRNA and VA RNA binding differentially. Alternatively, the interference could be more passive, for example, by preventing a conformational change in PKR that can be induced by dsRNA binding and is essential for activation. The bent shape of the VA RNA model, which is angled at the central domain in a fashion reminiscent of the tRNA L-shape or the 5S RNA "lollipop" (Kim et al., 1974; Van Ryk & Nazar, 1992), makes this second hypothesis an attractive one, but both views would be compatible with the unique structure of the central domain.

MATERIALS AND METHODS

Cells, viruses, and plasmids

Monolayer cultures of human 293 cells (Graham et al., 1977) and HeLa cells (ATCC CCL 2) were grown in Dulbecco's modified Eagle medium with 10% calf serum, and 100 μg of streptomycin and penicillin per milliliter as described (Ma & Mathews, 1993). Mutant virus Ad5*dl*331 (Thimmappaya et al., 1982) and wild-type adenovirus type 2 were grown in HeLa cells. The plasmids pAd2VAI, which expresses Ad2 VA RNA_I under its natural pol III promoter, and pSP6VAb, which expresses an antisense RNA probe for Ad2 VA RNA_I under the control of the SP6 promoter, were described previously (Ma & Mathews, 1993). The plasmid pT7VA, which expresses Ad2 VA RNA_I under the control of the phage T7 promoter, was described by Mellits et al. (1990b). Mutant pA2dl2 (Fowlkes & Shenk, 1980) was a gift of Dr. Tom Shenk. Mutant pMHVA*dl*1 was constructed by Mellits and Mathews (1988). Plasmids producing A2dl2 and *dl*1 RNAs under the control of the T7 promoter were constructed by Mellits et al. (1990b, 1992).

Mutagenesis of the VA RNA gene

Site-directed mutagenesis was performed following the method of Kunkel (Kunkel, 1985; Kunkel et al., 1987) to generate mutations in pT7VA and pAd2VAI. Oligonucleotides (5' to 3') CCATGATAGACTTGCGAA, CCATGATATTCTTGC GAA, and CCATGATAGCCTTGCGAA were used to make mutants L1, L2, and L3, respectively, and oligonucleotides CACACCTGTCTTCGACAC, CACACCTGAATTCGACAC, and CACACCTGGCTTCGACAC were used to make mutants R1, R2, and R3, respectively. To generate mutants L1-R1, L2-R2, L3-R3, and L1-R2, the appropriate L and R mutations were combined by isolating a *Kpn* I–*Bam*H I fragment containing the L mutations from pT7VA, or a *Sal* I–*Bam*H I fragment containing the L mutation from pAd2VAI, and inserting the isolated fragment in the same position in the R mutant clones.

Synthesis and end labeling of VA RNA

Transcription in vitro with T7 RNA polymerase was conducted as described previously (Mellits et al., 1990b, 1992). RNA was isolated by passing through Sephadex G-50 (medium) spin columns (Sambrook et al., 1989) twice, in STE buffer (0.15 M NaCl, 10 mM Tris-HCl, 1 mM EDTA, pH 7.4). RNA was labeled at its 5' end with [γ-^{32}P] ATP (ICN Radiochemicals, Inc.) or at its 3' end with [^{32}P]-pCp (ICN Radiochemicals, Inc.) as described (England & Uhlenbeck, 1978; Clarke & Mathews, 1995). Labeled RNA was resolved in a 5% sequencing gel and eluted from the excised gel slice by mixing for 2 h at room temperature with 300 μL STE in the presence of 50 μg calf liver tRNA and 30 μL Tris-saturated phenol.

Secondary structure analysis

Nuclease sensitivity analysis was conducted as described previously (Ma & Mathews, 1993; Clarke & Mathews, 1995). RNA was synthesized from the T7 constructs by T7 RNA polymerase, labeled at either its 5' or 3' end, and digested under conditions in which <10% of the molecules were cut. The nucleases used were RNase T_1, U_2, *Bacillus cereus* (Bc), and T_2, which cleave single-stranded regions at specific sites (G, A, pyrimidine, or any nucleotide, respectively), and nuclease V_1, which cleaves in regions of base paired and stacked

nucleotides. For RNase T_1, Bc, T_2, and V_1, the reaction conditions were 50 mM Tris·HCl, pH 7.5, 2 mM $MgCl_2$, and 150 mM KCl. RNase U_2 digests were conducted in 50 mM citric acid-potassium citrate buffer, pH 5.0, and 2 mM $MgCl_2$. For markers, RNA was treated with RNase T_1 at 68 °C or with alkali as described previously (Mellits & Mathews, 1988).

Translation rescue assay

The *dl*331 rescue assay (Larsson et al., 1986) was performed as described by Mellits and Mathews (1988). Human 293 cells, which had been passaged less than 10 times, were grown to about 60% confluency in 6-cm dishes. The cells were transfected with 5 μg of a plasmid construct containing a VA RNA gene and infected with Ad5*dl*331 at 24-h posttransfection (hpt). At 48 hpt, the cells were labeled for 1 h with ^{35}S-methionine (ICN Radiochemicals, Inc.) and 5% of the cytoplasmic extract was analyzed by electrophoresis in a 15% polyacrylamide/SDS gel. For northern blot analysis, RNA equivalent to 2–3% of the cells in a plate was resolved in a 1% agarose gel. The blot was probed with RNA complementary to the 5′ half of Ad2 VA RNA_1, labeled in transcription reaction with SP6 RNA polymerase, and purified through a 5% sequencing gel. Hybridization was performed as described previously (Ma & Mathews, 1993).

CAT expression enhancement assay

Human 293 cells were transfected with 6 μg of the chloramphenicol acetyltransferase (CAT) expression plasmid pβCAT-6.5 (Svensson & Akusjärvi, 1990), together with 7.5 μg of pAd2VAI, and labeled with ^{35}S-methionine as described previously (Ma & Mathews, 1993). A fraction (25%) of the cells was lysed in 0.25 M Tris, pH 8.0, buffer and assayed for CAT activity using [^{14}C] chloramphenicol (3,000 mCi/mmol; ICN Radiochemicals, Inc.) (Gorman et al., 1982). Acetylated chloramphenicol was separated by thin-layer chromatography and CAT activity was quantified using an AMBIS Radioisotope scanning system II. The other fraction (75%) of the cells was lysed in A buffer (0.14 M NaCl, 15 mM $MgCl_2$, and 0.5% Nonidet P-40) and 20% of this extract was kept for northern blot assay. From the remaining extract, equal radioactive counts were assayed for CAT protein synthesis by immunoprecipitation as described previously (Ma & Mathews, 1993). The labeled CAT protein was quantified with a Fuji bioimaging analyzer.

ACKNOWLEDGMENTS

We thank Tsafrira Pe'ery for advice and critical discussions. This work was supported by grant CA 13106 from the National Cancer Institute.

Manuscript accepted without revision August 1, 1996

REFERENCES

Akusjärvi G, Svensson C, Nygard O. 1987. A mechanism by which adenovirus virus-associated RNA_1 controls translation in a transient expression assay. *Mol Cell Biol 7*:549–551.

Barber GN, Wambach M, Thompson S, Jagus R, Katze MG. 1995. Mutants of the RNA-dependent protein kinase (PKR) lacking double-stranded RNA binding domain I can act as transdominant inhibitors and induce malignant transformation. *Mol Cell Biol 15*:3138–3146.

Chong KL, Feng L, Schappert K, Meurs E, Donahue TF, Friesen JD, Hovanessian AG, Williams BRG. 1992. Human p68 kinase exhibits growth suppression in yeast and homology to the translational regulator *GCN2*. *EMBO J 11*:1553–1562.

Clarke PA, Mathews MB. 1995. Interactions between the double-stranded RNA binding motif and RNA: Definition of the binding site for the interferon-induced protein kinase DAI (PKR) on adenovirus VA RNA. *RNA 1*:7–20.

Clarke PA, Pe'ery T, Ma Y, Mathews MB. 1994. Structural features of adenovirus 2 virus-associated RNA required for binding to the protein kinase DAI. *Nucleic Acids Res 22*:4364–4374.

Davies MV, Furtado M, Hershey JWB, Thimmappaya B, Kaufman RJ. 1989. Complementation of adenovirus virus-associated RNA I gene deletion by expression of a mutant eukaryotic translation initiation factor. *Proc Natl Acad Sci USA 86*:9163–9167.

England TE, Uhlenbeck OC. 1978. 3′-terminal labelling of RNA with T4 RNA ligase. *Nature 275*:560–561.

Fowlkes DM, Shenk T. 1980. Transcriptional control regions of the adenovirus VAI RNA gene. *Cell 22*:405–413.

Furtado MR, Subramanian S, Bhat RA, Fowlkes DM, Safer B, Thimmappaya B. 1989. Functional dissection of adenovirus VAI RNA. *J Virol 63*:3423–3434.

Ghadge GD, Malhotra P, Furtado MR, Dhar R, Thimmapaya B. 1994. In vitro analysis of virus-associated RNA1 (VAI RNA): Inhibition of the double-stranded RNA-activated protein kinase PKR by the VAI RNA mutants correlates with the in vivo phenotype and the structural integrity of the central domain. *J Virol 68*:4137–4151.

Ghadge GD, Swaminathan S, Katze MG, Thimmapaya B. 1991. Binding of the adenovirus VAI RNA to the interferon-induced 68 kDA protein kinase correlates with function. *Proc Natl Acad Sci USA 88*:7140–7144.

Gorman CM, Moffat LF, Howard BH. 1982. Recombinant genomes which express chloramphenicol acetyltransferase in mammalian cells. *Mol Cell Biol 2*:1044–1051.

Graham FL, Smiley J, Russell WC, Nairn R. 1977. Characteristics of a human cell line transformed by DNA from human adenovirus type 5. *J Gen Virol 36*:59–72.

Green SR, Manche L, Mathews MB. 1995. Two functionally distinct RNA binding motifs in the regulatory domain of the protein kinase DAI. *Mol Cell Biol 15*:358–364.

Green SR, Mathews MB. 1992. Two RNA binding motifs in the double-stranded RNA activated protein kinase, DAI. *Genes & Dev 6*:2478–2490.

Hershey JWB. 1989. Protein phosphorylation controls translation rates. *J Biol Chem 264*:20823–20826.

Hovanessian AG. 1989. The double stranded RNA-activated protein kinase induced by interferon: dsRNA-PK. *J Interferon Res 9*:641–647.

Hunter T, Hunt T, Jackson RJ, Robertson HD. 1975. The characteristics of inhibition of protein synthesis by double-stranded ribonucleic acid in reticulocyte lysates. *J Biol Chem 250*:409–417.

Jessen TH, Oubridge C, Teo CH, Pritchard C, Nagai K. 1991. Identification of molecular contacts between the U1 A small nuclear ribonucleoprotein and U1 RNA. *EMBO J 10*:3447–3456.

Judware R, Petryshyn R. 1991. Partial characterization of a cellular factor that regulates the double-stranded RNA-dependent eIF-2a kinase in 3T3-F442A fibroblasts. *Mol Cell Biol 11*:3259–3267.

Katze MG, DeCorato D, Safer B, Galabru J, Hovanessian AG. 1987. Adenovirus VAI RNA complexes with the 68,000 M_r protein kinase to regulate its autophosphorylation and activity. *EMBO J 6*:689–697.

Katze MG, Wambach M, Wong ML, Garfinkel M, Meurs E, Chong K, Williams BRG, Hovanessian AG, Barber GN. 1991. Functional expression and RNA binding analysis of the interferon-induced, double-stranded RNA-activated, 68,000-M, protein kinase in a cell-free system. *Mol Cell Biol 11*:5497–5505.

Kaufman RJ, Davies MV, Pathak VK, Hershey JWB. 1989. The phosphorylation state of eucaryotic initiation factor 2 alters translational efficiency of specific mRNAs. *Mol Cell Biol 9*:946–958.

Kaufman RJ, Murtha P. 1987. Translational control mediated by eukaryotic initiation factor-2 is restricted to specific mRNAs in transfected cells. *Mol Cell Biol 7*:1568–1571.

Kim SH. 1978. Crystal structure of yeast $tRNA^{phe}$, its correlation to the solution structure and functional implications. In: Altman S, ed. *Transfer RNA*. Cambridge, Massachusetts/London: The MIT Press. pp 248–293.

Kim SH, Suddath FL, Quigley FL, McPherson A, Sussman JL, Wang AHJ, Seeman NC, Rich A. 1974. Three-dimensional tertiary structure of yeast phenylalanine transfer RNA. *Science 185*:435–440.

Kitajewski J, Schneider RJ, Safer B, Munemitsu SM, Samuel CE, Thimmappaya B, Shenk T. 1986. Adenovirus VAI RNA antagonizes the antiviral action of interferon by preventing activation of the interferon-induced eIF-2a kinase. *Cell 45*:195–200.

Koromilas AE, Roy S, Barber GN, Katze MG, Sonenberg N. 1992. Malignant transformation by a mutant of the IFN-inducible dsRNA-dependent protein kinase. *Science 257*:1685–1689.

Kostura M, Mathews MB. 1989. Purification and activation of the double-stranded RNA-dependent eIF-2 kinase DAI. *Mol Cell Biol 9*:1576–1586.

Kunkel TA. 1985. Rapid and efficient site-specific mutagenesis without phenotypic selection. *Proc Natl Acad Sci USA 82*:488–492.

Kunkel TA, Roberts JD, Zakour RA. 1987. Rapid and efficient site-specific mutagenesis without phenotypic selection. *Methods Enzymol 154*:367–382.

Larsson S, Bellett A, Akusjärvi G. 1986. VA RNAs from avian and human adenoviruses: Dramatic differences in length, sequence, and gene location. *J Virol 58*:600–609.

Lee SB, Esteban M. 1994. The interferon-induced double-stranded RNA-activated protein kinase induces apoptosis. *Virology 199*: 491–496.

Li J, Petryshyn RA. 1991. Activation of the double-stranded RNAa-dependent eIF-2a kinase by cellular RNA from 3T3-F442A cells. *Eur J Biochem 195*:41–48.

Ma Y, Mathews MB. 1993. Comparative analysis of the structure and function of adenovirus virus-associated RNAs. *J Virol 67*:6605–6617.

Ma Y, Mathews MB. 1996. The structure, function, and evolution of adenovirus VA RNA: A phylogenetic approach. *J Virol*. Forthcoming.

Maitra RK, McMillan NAJ, Desai S, McSwiggen J, Hovanessian AG, Sen G, Williams BRG, Silverman RH. 1994. HIV-1 TAR RNA has an intrinsic ability to activate interferon-inducible enzymes. *Virology 204*:823–827.

Manche L, Green SR, Schmedt C, Mathews MB. 1992. Interactions between double-stranded RNA regulators and the protein kinase DAI. *Mol Cell Biol 12*:5238–5248.

Maran A, Mathews MB. 1988. Characterization of the double-stranded RNA implicated in the inhibition of protein synthesis in cells infected with a mutant adenovirus defective for VA RNA_1. *Virology 164*:106–113.

Mathews MB, Shenk T. 1991. Adenovirus virus-associated RNA and translational control. *J Virol 65*:5657–5662.

McCormack SJ, Thomis DC, Samuel CE. 1992. Mechanism of interferon action: Identification of a RNA binding domain within the N-terminal region of the human RNA-dependent P1/eIF-2a protein kinase. *Virology 188*:47–56.

Mellits KH, Kostura M, Mathews MB. 1990a. Interaction of adenovirus VA RNA_1 with the protein kinase DAI: Non-equivalence of binding and function. *Cell 61*:843–852.

Mellits KH, Mathews MB. 1988. Effects of mutations in stem and loop regions on the structure and function of adenovirus VA RNA_1. *EMBO J 7*:2849–2859.

Mellits KH, Pe'ery T, Manche L, Robertson HD, Mathews MB. 1990b. Removal of double-stranded contaminants from RNA transcripts: Synthesis of adenovirus VA RNA_1 from a T7 vector. *Nucleic Acids Res 18*:5401–5406.

Mellits KH, Pe'ery T, Mathews MB. 1992. Role of the apical stem in maintaining the structure and function of adenovirus virus-associated RNA stem. *J Virol 66*:2369–2377.

Meurs EF, Galabru J, Barber GN, Katze MG, Hovanessian AG. 1993. Tumor suppressor function of the interferon-induced double-stranded RNA-activated protein kinase. *Proc Natl Acad Sci USA 90*:232–236.

Minks MA, West DK, Benvin S, Baglioni C. 1979. Structural requirements of double-stranded RNA for the activation of 2',5'-oligo(A) polymerase and protein kinase of interferon-treated HeLa cells. *J Biol Chem 254*:10180–10183.

O'Malley RP, Duncan RF, Hershey JWB, Mathews MB. 1989. Modification of protein synthesis initiation factors and shut-off of host protein synthesis in adenovirus-infected cells. *Virology 168*:112–118.

O'Malley RP, Mariano TM, Siekierka J, Mathews MB. 1986. A mechanism for the control of protein synthesis by adenovirus VA RNA_1. *Cell 44*:391–400.

Pathak VK, Schindler D, Hershey JWB. 1988. Generation of a mutant form of protein synthesis initiation factor eIF-2 lacking the site of phosphorylation by eIF-2a kinases. *Mol Cell Biol 8*:993–995.

Pe'ery T, Mellits KH, Mathews MB. 1993. Mutational analysis of the central domain of adenovirus VA RNA mandates a revision of the proposed secondary structure. *J Virol 67*:3534–3543.

Pestka S, Langer JA, Zoon KC, Samuel CE. 1987. Interferons and their actions. *Annu Rev Biochem 56*:727–777.

Puglisi JD, Wyatt JR, Tinoco I Jr. 1988. A pseudoknotted RNA oligonucleotide. *Nature 321*:283–286.

Puglisi JD, Tan R, Calnan BJ, Frankel AD, Williamson JR. 1992. Conformation of the TAR RNA-arginine complex by NMR spectroscopy. *Science 257*:76–80.

Rahman A, Malhotra P, Dhar R, Kewalramani T, Thimmapaya B. 1995. Effect of single-base substitutions in the central domain of VAI RNA on its function. *J Viol 69*:4299–4307.

Reichel PA, Merrick WC, Siekierka J, Mathews MB. 1985. Regulation of a protein synthesis initiation factor by adenovirus virus-associated RNAI. *Nature 313*:196–200.

Sambrook J, Fritsch EF, Maniatis T. 1989. *Molecular cloning: A laboratory manual, 2nd ed*. Cold Spring Harbor Laboratory Press, Cold Spring Harbor, New York. p 152.

Samuel CE. 1991. Antiviral actions of interferon: Interferon-regulated cellular proteins and their surprisingly selective antiviral activities. *Virology 183*:1–11.

Schneider RJ, Safer B, Munemitsu SM, Samuel CE, Shenk T. 1985. Adenovirus VAI RNA prevents phosphorylation of the eukaryotic initiation factor 2 alpha subunit subsequent to infection. *Proc Natl Acad Sci USA 82*:4321–4324.

Sen GC, Taira H, Lengyel P. 1978. Interferon, double-stranded RNA, and protein phosphorylation. *J Biol Chem 253*:5915–5921.

Siekierka J, Mariano TM, Reichel PA, Mathews MB. 1985. Translational control by adenovirus: Lack of virus-associated RNA_1 during adenovirus infection results in phosphorylation of initiation factor eIF-2 and inhibition of protein synthesis. *Proc Natl Acad Sci USA 82*:1959–1963.

Strijker R, Fritz DT, Levinson AD. 1989. Adenovirus VAI-RNA regulates gene expression by controlling stability of ribosome-bound RNAs. *EMBO J 8*:2669–2675.

Svensson C, Akusjärvi G. 1985. Adenovirus VA RNA_1 mediates a translational stimulation which is not restricted to the viral mRNAs. *EMBO J 4*:957–964.

Svensson C, Akusjärvi G. 1990. A novel effect of adenovirus VA RNA_1 on cytoplasmic mRNA abundance. *Virology 174*:613–617.

Thimmappaya B, Weinberger C, Schneider RJ, Shenk T. 1982. Adenovirus VAI RNA is required for efficient translation of viral mRNAs at late times after infection. *Cell 31*:543–551.

Thomis DC, Samuel CE. 1993. Mechanism of interferon action: Evidence of intermolecular autophosphorylation and autoactivation of the interferon-induced, RNA-dependent protein kinase PKR. *J Virol 67*:7695–7700.

Van Ryk DI, Nazar RN. 1992. Effect of sequence mutations on the higher order structure of the yeast 5S rRNA. *J Mol Biol 226*:1027–1035.